Ecological Indicators 139 (2022) 108924

Contents lists available at ScienceDirect

Ecological Indicators

journal homepage: www.elsevier.com/locate/ecolind

Potential inhibition of the harmful dinoflagellate *Cochlodinium* (= *Margalefidinium*) *polykrikoides* by the intrusion of Changjiang diluted water into Korea coastal waters

Young Kyun Lim [a,b], Bum Soo Park [c], Su Ho Bak [d], Sang-Soo Baek [e], Seung Ho Baek [a,b,*]

[a] *Risk Assessment Research Center, Korea Institute of Ocean Science and Technology, Geoje 53201, Republic of Korea*
[b] *Department of Ocean Science, University of Science and Technology, Daejeon 34113, Republic of Korea*
[c] *Marine Ecosystem Research Center, Korea Institute of Ocean Science and Technology, Busan 49111, Republic of Korea*
[d] *IREMTECH Co., Ltd., 10-1, Busan 46079, Republic of Korea*
[e] *Department of Environmental Engineering, Yeungnam University, Gyeongsan 38541, Republic of Korea*

ARTICLE INFO

Keywords:
Changjiang diluted water (CDW)
CDW intrusion strength
Niño 3.4 index
Typhoon passage
Cochlodinium (=*Margalefidinium*) *polykrikoides*
Bloom scale

ABSTRACT

During the summer monsoon, a large amount of the Changjiang River discharge (CRD) extends into Korean coastal waters (KCWs) in the East China Sea, forming Changjiang diluted water (CDW). The harmful dinoflagellate *Cochlodinium* (=*Margalefidinium*) *polykrikoides* frequently causes massive blooms during the monsoon period, and these result in extensive economic losses in southern KCWs. We hypothesized that the scale of *C. polykrikoides* blooms can be varied depending on the intrusion strength of CDW into KCWs. We analyzed long-term (20 years) data (physicochemical factors and *C. polykrikoides* bloom area and duration) to test this hypothesis. In confirming the variability in annual salinity, the average Niño 3.4 index in the preceding winter was found to be positively correlated with the CRD in the following summer ($R^2 = 0.203$, $p < 0.05$). However, the surface salinity in our study area was not significantly correlated with the CRD ($p > 0.05$), indicating that not all of the CDW volume enters the southern KCWs. This incomplete transfer of CDW into KCWs was related to the path of typhoons in the East Asian region; typhoons are able to moderate the influence of CDW through strong water mixing between the upper and bottom layers. We found that the scale of *C. polykrikoides* blooms in KCWs was negatively correlated with the strength of the CDW intrusion. Together with previous and present findings, the influx of low salinity CDW can accelerate a rise in surface temperature, and this elevated temperature condition which is unfavorable for *C. polykrikoides* growth may lead to reductions in the scale of this dinoflagellate blooms. Our findings suggest that intrusion strength of CDW into KCWs plays important role in regulating *C. polykrikoides* population dynamics by causing inhibitory conditions.

1. Introduction

Global warming has caused unprecedented climate changes, mainly related to temperature, precipitation, and wind, as a result of interactions between the atmosphere and the oceans (Wells et al., 2015). The phytoplankton community, including harmful algal bloom (HAB) organisms, significantly responds to these environmental changes; the structure and composition of phytoplankton populations and their temporal and spatial distribution are varied (Hallegraeff, 2010; Paerl et al., 2010). Over recent decades the occurrence, frequency, and distribution of HABs have consistently increased, and HAB events have become an important global issue. HABs cause large economic losses in the aquaculture industry, and pose a serious threat to public health and aquatic sustainability (Kudela and Gobler, 2012). In particular, the ichthyotoxic unarmored dinoflagellate *Cochlodinium* (=*Margalefidinium*) *polykrikoides* is responsible for massive fish mortality, and blooms of this organism are increasingly threatening coastal ecosystems globally (Kudela and Gobler, 2012; Lee et al., 2013; Park et al., 2013). Since this dinoflagellate causes mass mortality of caged fish in Korean coastal waters (KCWs) during summer (Park et al., 2013), numerous studies have been performed to elucidate the factors affecting bloom dynamics in this area. Based on previous findings, physicochemical factors play a key role in the formation and termination of blooms (Baek et al., 2020a; Lee et al., 2016; Lee, 2006; Lim et al., 2015; Lim et al., 2019; Lim et al.,

* Corresponding author at: Risk Assessment Research Center, Korea Institute of Ocean Science and Technology, Geoje 53201, Republic of Korea.
E-mail address: baeksh@kiost.ac.kr (S.H. Baek).

https://doi.org/10.1016/j.ecolind.2022.108924
Received 6 February 2022; Received in revised form 7 April 2022; Accepted 25 April 2022
Available online 29 April 2022

2021).

The physiochemical conditions in KCWs are strongly affected by the introduction of water carried to the area by ocean currents (Lie and Cho, 2016; Lie and Cho, 1994). Southern KCWs are affected by ocean currents including the Jeju Warm Current and the Tsushima Warm Current, which is a branch of the Kuroshio Current and is characterized by high salinity (Lie and Cho, 2016; Lie and Cho, 1994). In addition, the Changjiang diluted water (CDW), formed by Changjiang River discharge (CRD) during the summer monsoon, enters southern KCWs from the East China Sea. It is characterized by low salinity and high temperature, and is capable of affecting physicochemical condition in the receiving area (Bai et al., 2014). In addition, the CDW can cause variation in other environmental conditions, such as the concentrations of nutrients and dissolved oxygen (Jiang et al., 2014; Liu et al., 2018), with the extent of its influence dependent on the volume of water introduced.

The amount of CDW intrusion into KCWs can be determined by levels of the two factors; the initial formation of CDW and the transport of the formed CDW. First, as a source, the initial amount of CDW is most affected by precipitation in the Changjiang River basin and amount of the CRD. According to Park et al. (2015), the amount of the CRD is closely associated to El Niño–Southern Oscillation (ENSO)-related precipitation over the Changjiang River. Based on an ocean general circulation model (OGCM), in case of occurrence of an El Niño event in winter, the amount of the CRD was elevated during summer in the following year. In addition, as a transport, a second potential influencing factor is vertical mixing caused by the passage of typhoons. It is well known that typhoons (tropical cyclones) are one of the most energetic meteorological phenomena in the marine environment. Typhoon-induced strong winds cause vertical mixing of water mass, which can alter typical CDW extension patterns. The previous studies found that changes in the direction and the amount of CDW extension into KCWs after the passage of typhoons through the in situ measurement and numerical simulation (Lee et al., 2017; Zhang et al., 2018). Given these findings, the passage of typhoons can be an important factor, determining the amount of CDW intrusion into KCWs along with the CRD, but this is unclear due to lack of evidence. Thus, it is necessary to examine this relationship using long-term historical data.

The intrusion of CDW, which varied annually, can have major impacts on marine organisms in KCWs, particularly the mass mortality of macro-benthic organisms around Jeju Island (Suh et al., 1998). In addition, there has been much debate about impact of the summer intrusion of CDW on *C. polykrikoides* blooms, even though these two events occurred, simultaneously. Lee et al. (2016) and Lee (2008) suggested that the influx of CDW may create favorable environmental conditions for the occurrence of *C. polykrikoides* blooms, including cell aggregation and the supply of abundant nutrients. Whereas, Park et al. (2019) suggested that changes in the N/P ratio are associated with a negative relationship between the abundance of *C. polykrikoides* and the CRD. Although these studies have discussed the relationship between *C. polykrikoides* blooms and CDW, there has been little study of annual variations in the CDW intrusion and the effect of these on the scale of *C. polykrikoides* blooms, including their area and duration.

We hypothesized that the scale of *C. polykrikoides* blooms could be affected by variation in the extent of intrusion of CDW into KCWs. To test this hypothesis, we first analyzed long-term physicochemical environmental data to determine the annual strength of the CDW intrusion into southern KCWs. Second, the effect of ENSO index and typhoon passage on initial formation and transport of CDW intrusion into southern KCWs was elucidated using long-term historical data. Finally, we examined the relationship between the CDW intrusion into southern KCWs and the scale of *C. polykrikoides* blooms.

2. Materials and methods

2.1. The study area and collection of hydrological data

Since the mid-1990s, monitoring has been carried out six times per year (February, April, June, August, October, December) in the Yellow Sea, the East Sea (Sea of Japan), and southern KCWs, and four times per year in the East China Sea, under the Serial Oceanographic Observation Program of the NIFS (National Institute of Fisheries Science). Environmental parameters including water temperature, salinity, the dissolved oxygen (DO) concentration, and the concentrations of dissolved inorganic nutrients (nitrite + nitrate; NO_x, phosphate, and silicate) have been measured as part of the program, and the resulting data are archived by the NIFS (http://www.nifs.go.kr/kodc). To investigate salinity gradient changes caused by CDW intrusion, the study area was divided into two zones (zones I and II) based on the distance from the southern Korean coast (Fig. 1) on longitude 126.2°E (left border of Jeju Island).

The data used focused on sites corresponding to the CDW intrusion pathway (Bai et al., 2014), except for the distribution of annual surface

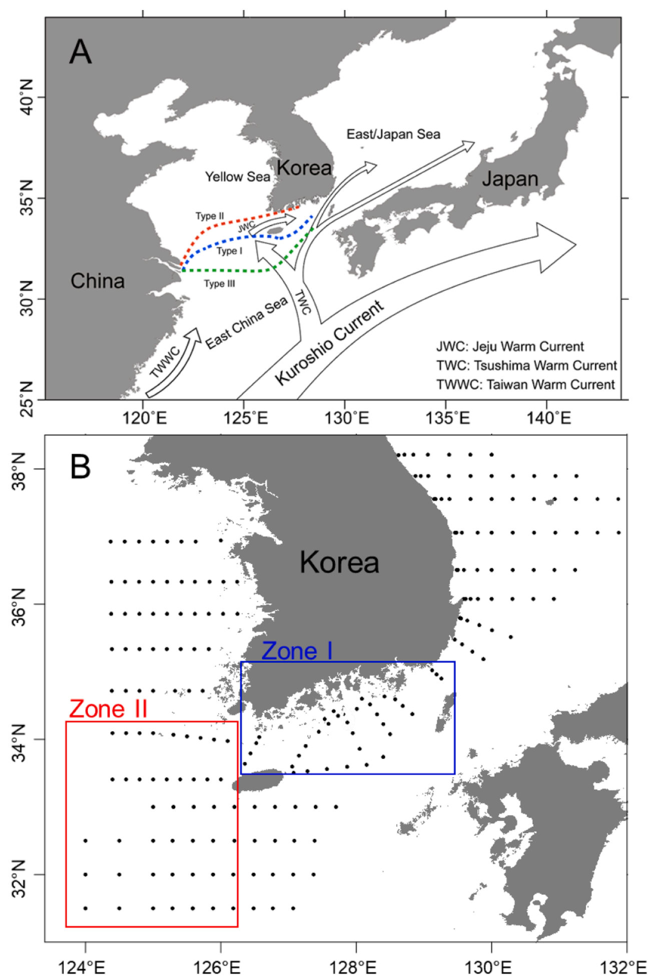

Fig. 1. The study area. A: Location of the Korean Peninsula, and patterns of surface currents in the northwestern Pacific marginal seas. CDW: Changjiang Diluted Water (the colored dashed lines indicate various types of CDW intrusion, as described by Bai et al., 2014. Blue: type I; red: type II; green: type III); TWWC: Taiwan Warm Current; JWC: Jeju Warm Current; TWC: Tsushima Warm Current. B: sampling sites for the Serial Oceanographic Observation Program of National Institute of Fisheries Science. The colored boxes indicate the zones used for analyzing the influence of CDW (blue: zone I; red: zone II). Zones were separated according to distance from the southern Korean coastal line, based on longitude 126.2°E (left border of Jeju Island).

salinity in August (Fig. 2A). Only data (water temperature, salinity, DO and dissolved inorganic nutrients) for surface waters in August were used in comparisons of water conditions in relation to the strength of CDW intrusion into southern KCWs from 1994 to 2016. Classification of the annual intrusion of CDW into southern KCWs was based on the salinity in each zone, and years having strong and weak CDW intrusions were selected based on the absolute value of *Z*-scores. The *Z*-scores were calculated based on the annual average salinity in each zone, and was determined using the equation:

$$Z-\text{score} = \frac{X_i - \overline{X}}{\sigma}$$

where X_i is the average salinity for each year, and $\overline{X}$ (mean value) and σ (standard deviation) were calculated from the entire dataset in each zone. The years having strong CDW intrusion (Z-score $>\ -1$) were 1996, 2005, 2006, 2010, and 2016, while the weak CDW intrusion years (Z-score $< +1$) were 1994, 1995, 1999, 2002, 2011, and 2014 (Fig. 3C).

2.2. Duration and cumulative area of *C. polykrikoides* blooms

Red tide monitoring in Korea has been conducted by the NIFS since 1972, and a nationwide red tide monitoring network was established in 1995 following a massive fish kill caused by *C. polykrikoides* blooms (Lee et al., 2013). Monitoring for early detection and warning of *C. polykrikoides* blooms is conducted at two-week intervals from June to October, using field surveys along the southern coast of Korea (Lee et al., 2013). When a red tide occurs, a daily red tide newsletter is published that includes cell density and location information, and predictive information about the development and extinction of the red tide is made available at the NIFS red tide management system data (http://www.nifs.go.kr/rtm/TRS/gispop/redtide.jsp). To determine the duration of *C. polykrikoides* blooms in each year we used the daily red tide data from the NIFS red tide management system (Table 1). In addition, the georeferencing data (locations where blooms occurred) from 2000 to 2016 in the NIFS red tide management system were used to determine the cumulative bloom area. Since data for 2004 and 2006 were absent in the NIFS red tide management system, these two years (2004 and 2006) data were excluded when we analyzed bloom area. Georeferencing was accomplished by superimposing latitude/longitude data onto an aerial photograph or map lacking geographic coordinates. In this case, the coordinates of the entire map may be obtained by estimating the geographical coordinates of the remaining non-overlapping areas based on the same region on the two maps. As the red tide area map is provided in image format (jpg, png), the objects on the map were projected in the x and y coordinate system. A ground control point (GCP) was selected for each map, and matched with the digital map that included the geographic coordinate system. All other coordinates were added as relative coordinates with respect to the reference point (the GCP); the geodetic datum used was WGS84 (World Geodetic System 1984). To calculate the area, the red tide area was digitized to a polygon from the georeferenced red tide area map, and the inner area of the polygon was used as the area of the red tide.

2.3. El Niño–Southern Oscillation, Changjiang River discharge

The sources of data on the ENSO and the CRD are shown in Table 1. Sea surface temperature (SST) anomalies in the Niño 3.4 region (5°S–5°N, 90–150°W), representing the ENSO, were obtained from the National Oceanic and Atmospheric Administration (https://psl.noaa.gov/gcos_wgsp/Timeseries/Nino34). Based on the time-delayed correlation between ENSO and precipitation over the Changjiang River by Park et al., (2015), the preceding winter (December–January–February: DJF) Niño 3.4 SST anomalies, averaged over the Niño 3.4 region, were used for correlation with the CRD and salinity to study the effect of ENSO on the CRD in summers over the period 1994 to 2016. The CRD data were based on measurements made without tidal influence at the Datong hydrological gauge station, which is located 624 km upstream from the Changjiang River mouth.

2.4. Path of typhoon and economic losses caused by *C. polykrikoides* bloom

To investigate the effect of typhoons on the intrusion of CDW into southern KCWs, the paths of typhoons from 1 July to 20 August in strong and weak CDW years were traced, based on data from the Korea Meteorological Administration (KMA; https://www.weather.go.kr/weath

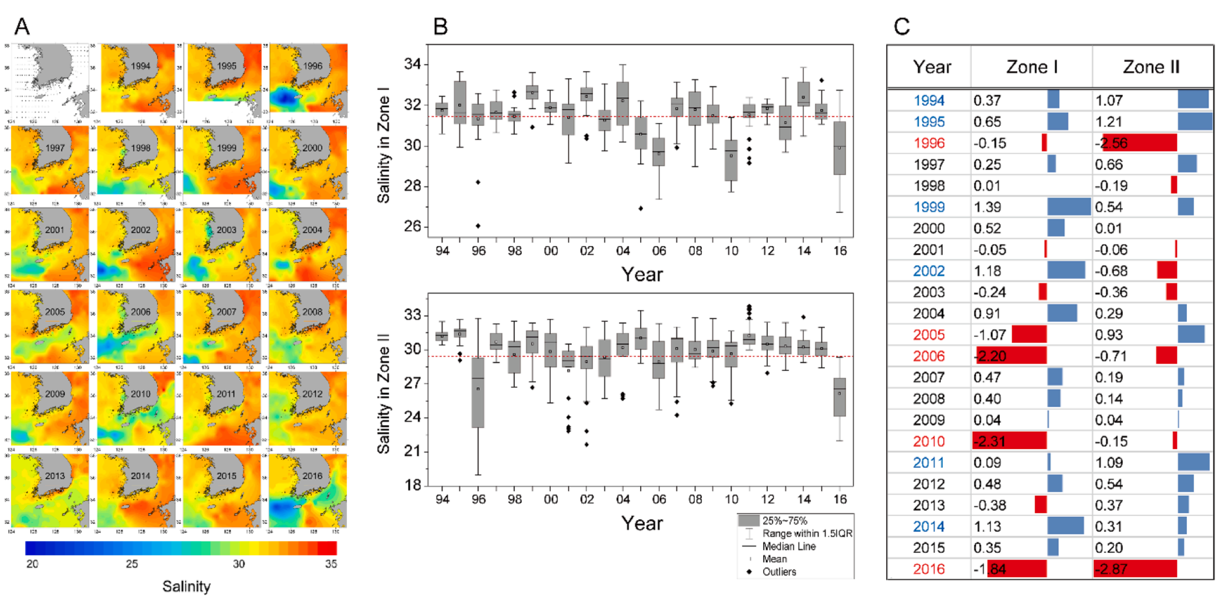

Fig. 2. Annual variation of surface salinity in the study area in August 1994–2016. A: Horizontal distribution of surface salinity in the study area in August 1994–2016. B: Annual variation in surface salinity in each zone (Top: Zone I; Bottom: Zone II) in August 1994–2016; The red dashed line indicates the average salinity in each zone over the 23 years. C: Annual *Z*-scores for each zone, used in classifying the strength of the intrusion of CDW into southern Korea coastal waters. The years categorized as strong and weak CDW were selected based on the absolute value of *Z*-scores exceeding 1. Blue and red text and highlighting indicate weak and strong CDW years, respectively.

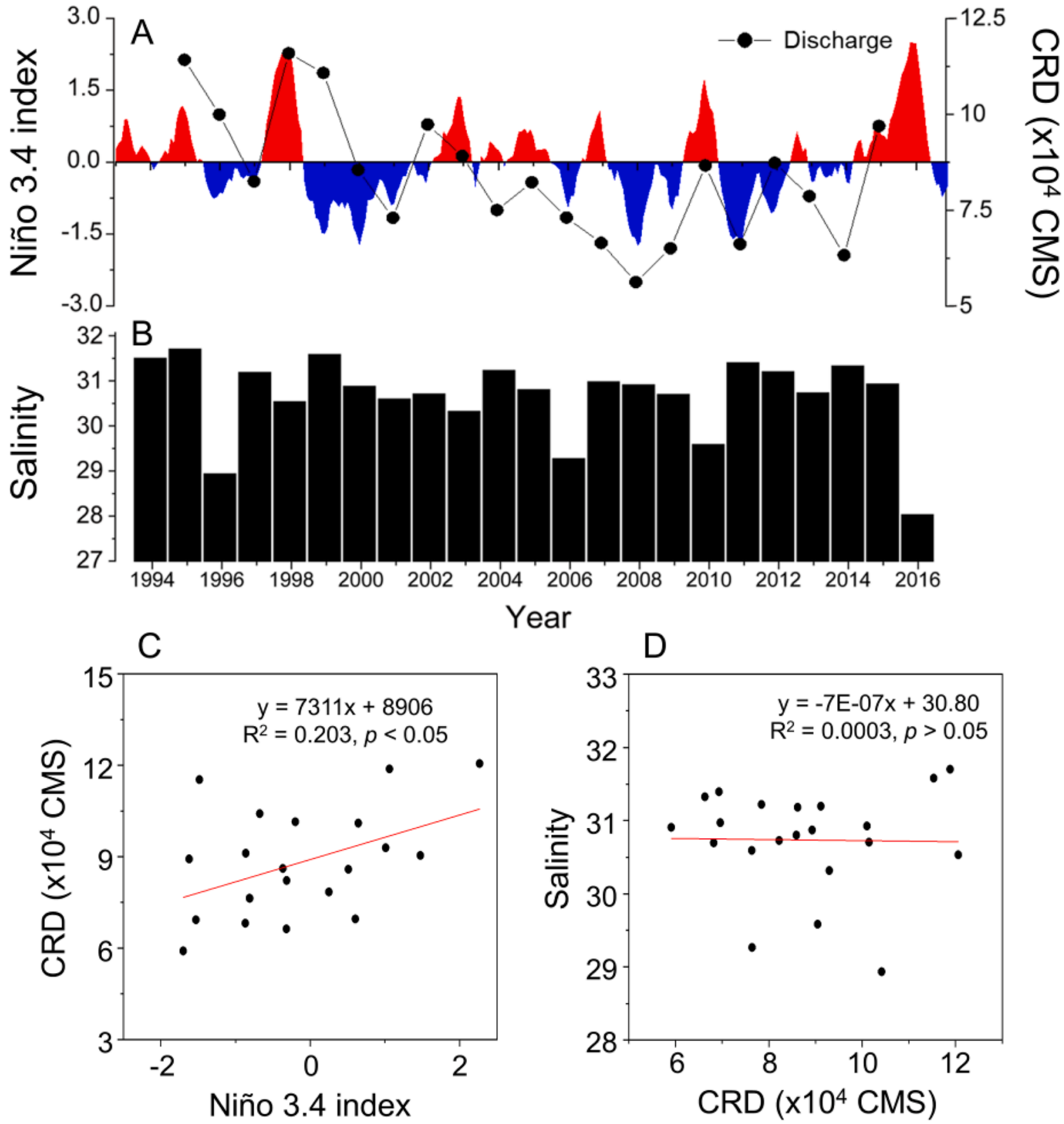

Fig. 3. Annual variations of, and relationships among, environmental parameters during the study period. A: Annual variation in the Niño 3.4 SST (sea surface temperature; red and blue hatched areas represent the positive and negative anomalies, respectively) and the Changjiang River discharge (CRD; black line and circle symbols). B: Average surface salinity in August in both zones (black bar graph). Relationships between: The Niño 3.4 index and the CRD (C); and the CRD and salinity (D). The Niño 3.4 index used to assess relationships with other factors were the average Niño 3.4 SST anomalies in the preceding winter (December–January–February; DJF) from 1994 to 2016. Linear regression lines (red) and R^2 and p values are also shown.

er/typoon). Data on annual (2000–2016) economic losses caused by *C. polykrikoides* blooms were obtained from the Ministry of Oceans and Fisheries (https://www.mof.go.kr/article/view.do?menuKey=427&boardKey=2&articleKey=26880).

2.5. Statistical analysis

All statistical analyses were performed using SPSS software version 23 (SPSS Inc.; Chicago, IL, USA). Linear regression analysis was performed to assess the correlations among variables including: (i) between salinity (representing the strength of CDW intrusion into KCWs) and factors affecting the CDW volume (Niño 3.4 index, CRD); (ii) between sigma-t and *C. polykrikoides* bloom parameters (duration and cumulative area; a logarithmic scale was used for cumulative area because of the large variations from the other parameter); and (iii) between properties of *C. polykrikoides* blooms (duration, daily bloom area, and cumulative bloom area) and economic losses. In addition, to assess environmental changes depending on the strength of CDW intrusion into southern KCWs, a student's *t*-test was used to compare environmental variables (water temperature, salinity, DO, inorganic nutrients: NO_x, phosphate, silicate) among strong and weak CDW years. For all analysis, differences were considered to be statistically significant at $p < 0.05$.

3. Results

3.1. Changes in the salinity distribution pattern in summer

During the 23 years of the study the horizontal distribution of salinity in surface waters in August varied markedly each year (Fig. 2A). Overall, the surface salinity around the Korean peninsula was highest in the East Sea (Sea of Japan), in the east of the study area (average: 32.8 ± 0.46), followed by the Yellow Sea in the west, and southern KCWs and the East China Sea in the south. In this period a trend of low salinity (average: 30.6 ± 1.13) was observed in southern waters, including southern KCWs and the East China Sea, and the distribution of low saline water varied annually. In the two zones the average annual salinity ranged from 28.2 (2016) to 32.8 (2000), and in 74% of the 23 years the salinity fluctuated between 30 and 31. During the 23 years the average

Table 1
Sources of data used.

Factors	Source	Years
Temperature Salinity DO Nutrients	Korea Oceanographic Data Center (KODC) Serial Oceanographic Observation Program of National Institute of Fisheries Science (NIFS; http://www.nifs.go.kr/kodc)	1994–2016
Bloom area	NIFS red tide management system data (http://www.nifs.go.kr/rtm/TRS/gispop/redtide.jsp)	2000–2016 (unavailable in 2004 and 2006)
Bloom duration		2000–2016
Economic losses	Ministry of Oceans and Fisheries (https://www.mof.go.kr/article/view.do?menuKey=427&boardKey=2&articleKey=26880)	2000–2016
Changjiang River discharge	Yangtze River Water Conservancy Committee (https://www.cjh.com.cn)	1995–2015
Niño 3.4 index	National Oceanic and Atmospheric Administration (NOAA; https://psl.noaa.gov/gcos_wgsp/Timeseries/Nino34)	1994–2016
Path of typhoon	Korea Meteorological Administration (KMA; https://www.weather.go.kr/weather/typhoon)	Weak CDW years (1994, 1995, 1999, 2002, 2011, and 2014) and strong CDW years (1996, 2005, 2006, 2010, and 2016)

salinity in Zone I was 31.5 ± 0.8, and in Zone II was 29.8 ± 1.3 (Fig. 2B). In four of the weak CDW years in this period (2005, 2006, 2010, and 2016), the average salinity in Zone I was very low (average: 29.9 ± 0.4; Z-score < − 1; Fig. 2B and 2C). In Zone II, in only two years (1996, 2016) did the average salinity (26.5 ± 0.20) have a Z-score < − 2 (Fig. 2B and 2C). The average salinities in strong and weak CDW years (29.4 ± 2.4 and 31.3 ± 1.05, respectively) were significantly different (t-test, $p < 0.01$) (Table 2).

3.2. Annual variation and relationships among CDW-related factors

Fig. 3 shows the annual variations in the Niño 3.4 index, the CRD, and average salinity in Zone I and II, and their relationships as determined by linear regression. For Niño 3.4 index, positive SST anomalies occurred in 1995, 1998, 2003, 2005, 2007, 2013, and 2016, while the remaining years had negative SST anomalies (Fig. 3A). The volume of the CRD in June and July each year showed a similar pattern of variation as for Niño 3.4 index (yearly increase or decrease). In 1995, 1996, 1998, 1999, 2002, and 2015 the CRD exceeded 10^5 m^3 s^{-1} (CMS) (average 11.0 ± 0.8 × 10^4 CMS), whereas, in 2008, 2009, 2011, and 2014 it was < 7 × 10^4 CMS (average 6.6 ± 0.4 × 10^4 CMS). The average surface salinity in August over the 23 years was 30.7 ± 0.9; relatively low salinities (<30; average: 29.0 + 0.6) were recorded in four years (1996, 2006, 2010, and 2016) (Fig. 3B). Salinity did not show similar annual variability to Niño 3.4 index and the CRD. The average Niño 3.4 index in the preceding winter (DJF) was significantly positively correlated with the CRD in the following summer ($R^2 = 0.203$, $p < 0.05$; Fig. 3C), but not with salinity ($p > 0.05$). In addition, the CRD was not significantly correlated with the average salinity ($p > 0.05$; Fig. 3D).

Table 2
The results of t-test analysis between strong and weak CDW years for: temperature, salinity, dissolved oxygen (DO), dissolved inorganic nitrate + nitrite (NO_x), dissolved inorganic phosphate (DIP), and dissolved inorganic silicate (DSi).

		Mean	SD	t	p
Temperature (°C)	strong	27.95	1.89	18.89	0.00
	weak	25.40	1.94		
Salinity	strong	29.38	2.36	−13.57	0.00
	weak	31.30	1.49		
DO (mg L^{-1})	strong	5.19	0.67	5.03	0.00
	weak	4.97	0.45		
NO_x (μM)	strong	3.88	3.81	3.62	0.00
	weak	2.72	2.48		
DIP (μM)	strong	0.15	0.20	−0.19	0.85
	weak	0.15	0.22		
DSi (μM)	strong	5.31	3.53	−1.05	0.30
	weak	5.63	2.65		

3.3. Comparison of passage of typhoons between strong and weak CDW years

The number of typhoons in weak CDW years and strong CDW years during the summer were 22 and 27, respectively (Fig. 4). There was a clear difference in the number and rate of typhoons that passed through the study area between the weak and strong CDW years. In weak CDW years, 10 typhoons, accounting for 45 % of all typhoons, passed through the study area (Fig. 4A), including: Typhoon *Faya* on 23 July 1995; typhoons *Neil* (27 July), *Olga* (3 August), *Paul* (7 August) and *Rachel* (10 August) in 1999; typhoons *Nakri* (13 July) and *Fengshen* (26 July) in 2002, typhoon *Muifa* on 7 August 2011; and typhoons *Nakri* (2 August) and *Neoguri* (10 August) in 2014. In strong CDW years, 2 typhoons, accounting for 7 % of all typhoons, passed through the study area (Fig. 4B), including: Typhoon *Ewiniar* on 9 July 2006; and typhoon *Dianmu* on 10 August 2010.

3.4. Annual variations in the *C. polykrikoides* blooms and their relationship with sigma-t

Overall, the historical *C. polykrikoides* bloom area (1995–2016) was concentrated on the southern coast of Korea, and in nine years (1996, 1998, 2000, 2004, 2005, 2006, 2008, 2012, and 2016; 41% of the total number of years analyzed) red tides occurred only in southern KCWs (Fig. 5A). When red tides occurred over a wider area in the other ten years (1995, 1997, 1999, 2001, 2002, 2003, 2007, 2013, 2014, and 2015), the blooms tended to occur on both the southern and eastern coasts of Korea. The historical *C. polykrikoides* bloom area showed the spatial locations where red tides had occurred, whereas data on the cumulative bloom area and duration indicated the strength of annual *C. polykrikoides* blooms.

After 2000 the cumulative *C. polykrikoides* bloom area varied from 20 km^2 (2009) to 17,380 km^2 (2003) (Fig. 5B). From 2000 to 2002 there were large *C. polykrikoides* blooms having an average area of 6959 km^2, while 2003 had the largest cumulative bloom area among the years analyzed (17,380 km^2). For the next seven years (2005 to 2011), the blooms were small (average area: 522 km^2). However, over the next four years the *C. polykrikoides* blooms were large (3201 km^2, 7992 km^2, 2091 km^2, and 6378 km^2), averaging 5000 km^2. In 2016 the bloom area was extremely small (<100 km^2). During the 17 years the average duration of *C. polykrikoides* blooms was 33 days (Fig. 5B). In the nine years (2000, 2001, 2002, 2003, 2005, 2012, 2013, 2014, 2015) in which the bloom area was relatively large (>2000 km^2), the average duration was 47 days, which was two weeks longer than the average for the entire period. In 2003, when the largest cumulative bloom area (17,380 km^2) was recorded, the red tide lasted for a relatively short period (40 days), while in 2008 the bloom was small in area (775 km^2), but lasted for 55 days.

To investigate the effect of CDW intrusion on *C. polykrikoides* blooms in southern KCWs, we performed linear regression between properties of *C. polykrikoides* blooms (cumulative area and duration) and sigma-t, as an indicator of CDW intrusion (low sigma-t) into southern KCWs (Fig. 5C). The linear regression between sigma-t and cumulative bloom area showed a significant positive correlation ($R^2 = 0.29$, $p < 0.05$). In addition, the duration of *C. polykrikoides* blooms was positively correlated to sigma-t with higher significance ($R^2 = 0.42$, $p < 0.05$). The average duration and cumulative area of *C. polykrikoides* blooms in

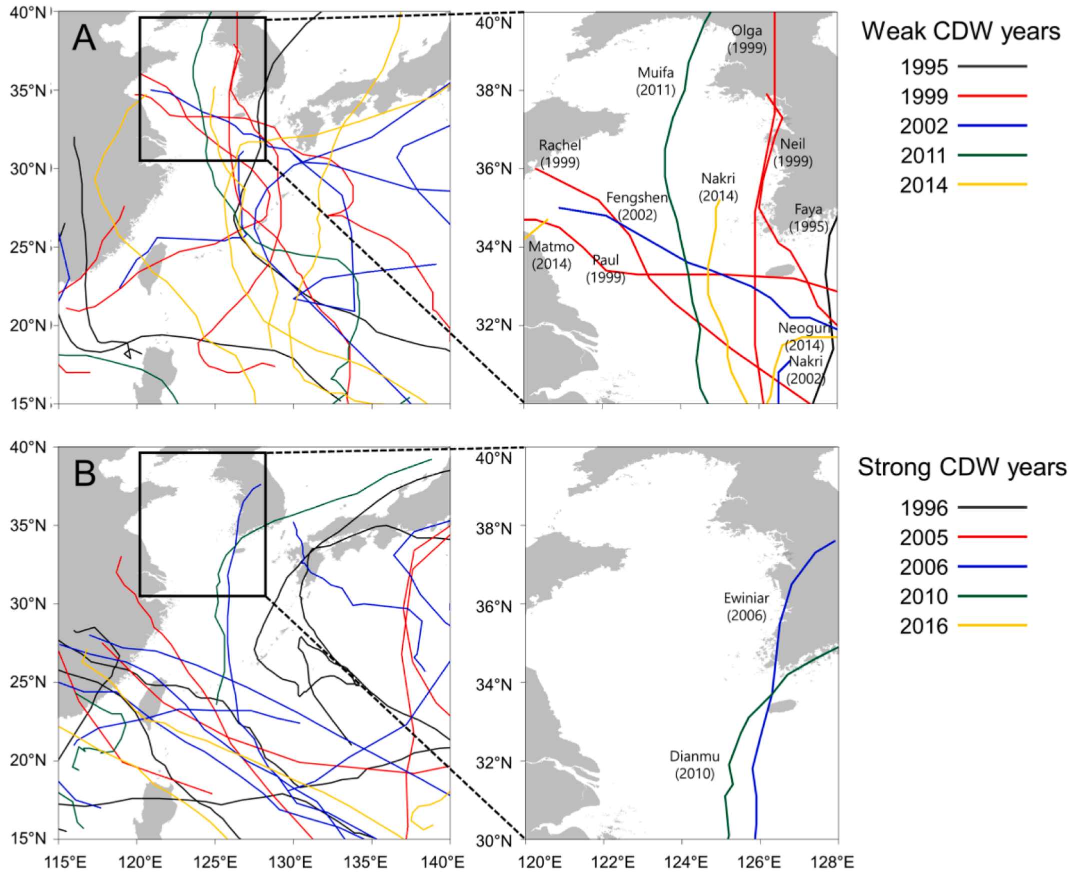

Fig. 4. Paths of typhoons (colored lines) passing the study area from 1 July to 20 August in weak (A) and strong (B) CDW years during the study period. The latitude and longitude ranges were 115–140°E and 15–40°N for left maps, and 120–128°E and 30–40°N for right zoomed maps.

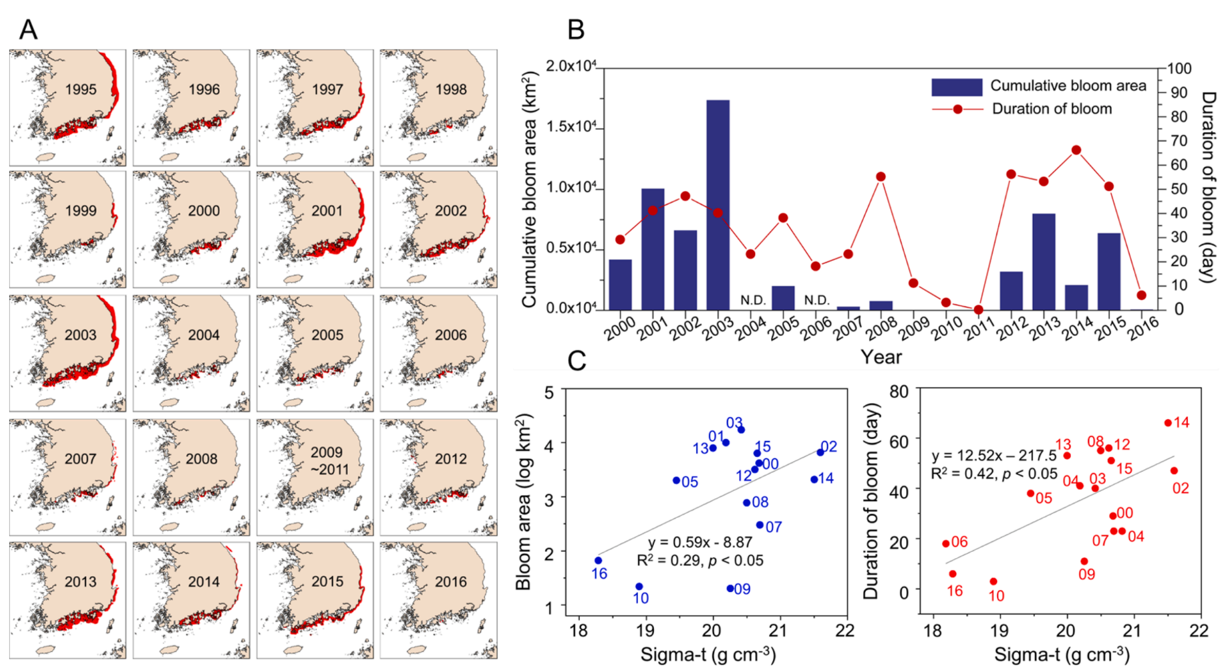

Fig. 5. Annual variations in the distribution and the scale of *C. polykrikoides* blooms and their relationship with sigma-t. A: Spatial distribution of *C. polykrikoides* blooms from 1995 to 2016 in Korean coastal waters. The original figure from which these were developed was provided by the Red Tide Control Room, NIFS. B: Annual variation in the cumulative area (blue bar graph) and duration (red circled symbol and line graph) of *C. polykrikoides* blooms from 2000 to 2016 (the cumulative areas of the blooms in 2004 and 2006 were unavailable). C: Relationship between the sigma-t in Zone I and the scale of *C. polykrikoides* bloom (Cumulative bloom area: left blue, duration: right red figure); The numbers in the graph indicate the year.

strong CDW years with sigma-t less than 19.5 g cm^{-3} were 16 days and 701 km^2 (Fig. 5C). Whereas, the average duration and cumulative area of the blooms in weak CDW years (except 2011) with sigma-t over than 21 g cm^{-3} were 57 days and 4354 km^2.

3.5. Relationship between the scale of *C. polykrikoides* blooms and economic losses

The economic losses caused by *C. polykrikoides* blooms after 2000 was the highest at 22.5 million USD in 2013, followed by 19.5 million USD in 2003 (Fig. 6). The average economic losses in weak CDW years was 5.7 million USD (excluding 2011 when no bloom). On the other hand, the economic losses in strong CDW years was small, with an average of 0.3 million USD. The economic losses showed a significant correlation only with the latter among the bloom duration and area ($R^2 = 0.41$, $p < 0.05$). In addition, the cumulative bloom area, a parameter that includes the bloom duration, showed a significant positive correlation with economic losses ($R^2 = 0.53$, $p < 0.05$).

4. Discussion

4.1. Extension of CDW into southern KCWs

Large volumes of the CRD markedly affect Chinese coastal waters during the summer monsoon, related to extensive precipitation and runoff from China (Wei et al., 2015). The CDW, formed by mixing of river runoff and coastal waters, extends northeast under the influence of southerly winds and oceanic currents to the Tsushima–Korea strait during summer, and reaches southern KCWs with a time lag of 1–2 months (Bai et al., 2014; Kim et al., 2009). Because of this process, the amount of the CRD is a very important factor affecting the total volume of CDW entering southern KCWs. In summer, the amount of the CRD is determined by precipitation in the Changjiang River catchment. The summer monsoon weakens with warming of tropical waters; this affects the convergence of water vapor over southern China, and increases precipitation in the Changjiang River basin (Li et al., 2010; Zhou et al., 2008). Anomalies in the SST in the central equatorial Pacific (the Niño 3.4 region), which are reflected in the Niño 3.4 SST index, can affect the CRD by influencing the strength of the summer monsoon. A recent study based on the global OGCM has demonstrated that an increase in water temperature in tropical waters in winter can subsequently lead to an increase in precipitation in southern China, and result in increased the CRD in the following summer (Park et al., 2015). In the present study the average Niño 3.4 index in the preceding winter (DJF) was positively correlated with the amount of the CRD in the following summer (sum of June and July) ($p < 0.05$). Given these findings, elevation of the amount of the CRD may lead to increase in the amount of CDW, resulting in a decrease of the salinity level in southern KCWs. However, the average salinity, which indirectly reflects the influence of CDW, was not significantly correlated with the Niño 3.4 index and the CRD ($p > 0.05$). These results indicate that initial formation of CDW was heavily influenced by increased precipitation in China, whereas all of the CDW volume was not completely introduced into the southern KCW.

The influence of external forcing can be considered as the reason for the incomplete introduction of CDW into southern KCWs. The passage of typhoons in summer plays an important role in determining vertical mixing of water masses, even in strongly stratified water column environments (Baek et al., 2018; Baek et al., 2020b; Chen et al., 2009). Zheng and Tang (2007) reported that 40% of typhoons in western Pacific regions pass through the South China Sea, and the remaining 60% impact the East China Sea and East Asian countries; 14% of these directly or indirectly influence the Korean Peninsula. According to Bai et al. (2014), from 1998 to 2010 the average annual geographic spread of the CDW plume was 3.3 ± 0.5 × 10^5 km^2, and because of its low density the plume floats on the surface layer (approximately 20 m depth) (Matsuno et al., 2006). Therefore, extensive water mixing caused by typhoons is likely to reduce the spread of CDW before it enters southern KCWs, particularly in Zone I. Zhang et al. (2018) reported that the expansion path and strength of CDW have been significantly altered by wind-driven current and wave-induced mixings after the passage of typhoon *Chanhom* in early July. In addition, Lee et al. (2017) reported that typhoon *Ewiniar* in 2006 and typhoon *Dianmu* in 2010 weakened the expansion of the CDW by water mixing. These studies suggested that 2–3 weeks' period is necessary to recover to the original low salinity level after typhoon passage, resulting in delay the inflow of CDW into KCWs. During weak and strong CDW years, the occurrence and path of typhoons tended to be concentrated in weak CDW years in our study area (north of the East China Sea and near Jeju Island) (Fig. 4). In addition, the average CRD in 1995, 1999, and 2002 was very high (11.2 ± 0.75 × 10^4 CMS), but the level of salinity was also relatively high, suggesting only a small effect of CDW. Conversely, only two typhoons (typhoon *Ewiniar* in 2006 and typhoon *Dianmu* in 2010) passed through the study area during strong CDW years (Fig. 4B). Although both typhoons were analyzed as contributing to CDW attenuation by Lee et al., (2017), both years (2006, 2010) were classified as strong CDW years in our analysis. Considering the recovery period (2–3 weeks) of CDW proposed by Lee et al. (2017) and Zhang et al. (2018), the passage time of typhoons can act as an important factor in the low salinity effect of KCWs in August. Among the tracked typhoons during weak CDW years, at least one typhoon passed the study area (latitude: 30–40°N, longitude: 120–128°E) from the end of July to the beginning of August. Since there were no other typhoons after typhoon *Ewiniar* passed in early July 2006, the time remaining until August is considered sufficient for CDW recovery. Whereas, typhoon *Dianmu* passed in early August when CDW was not sufficient for recovery, which could lead to weakening of the inflow to southern KCWs. The Three Gorges Dam (TGD), the world's biggest dam, was built on Changjiang River in 2003 (Gao et al., 2013). The level of the CRD remarkably decrease in accordance with TGD

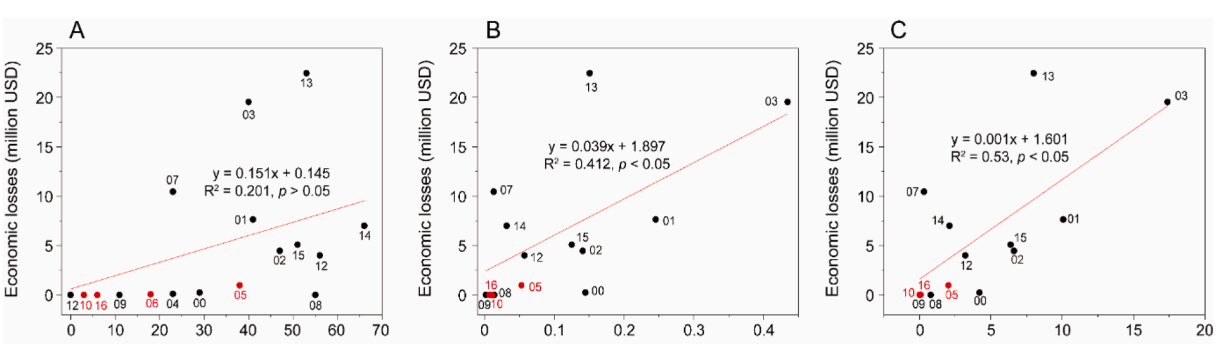

Fig. 6. The relationship of economic losses caused by *C. polykrikoides* blooms since 2000 and (A) the duration of blooms, (B) the bloom area per day, and (C) the cumulative bloom area. Linear regression (red) lines and R^2 and p values are also shown. Red symbols and letters indicate strong CDW years.

construction (Gao et al., 2013; Mei et al., 2015; Yang et al., 2015). In particular, during the wet period, a 7.4% decrease in the CRD was reported in post-TGD decade (2003–2012) compared to pre-TGD decade (1993–2002) (Yang et al., 2015). During the same post-TGD period, the amount of the CRD in 2010 was about 1.3 times greater than in the weak CDW years in 2011 and 2014. This relatively large amount of the CRD in 2010 may allow to overcome the CDW disturbance by the typhoon and led to the rapid recovery of CDW. In 2020 a record high level of precipitation in China caused an extremely destructive flood, resulting in a large CRD. As a result, CDW at a salinity < 26 to a depth of 10 m affected Jeju Island (22 August 2020), but with the passage of typhoon *Bavi* on 27 August the low salinity water (CDW) immediately dissipated (KMA 2020 report; Korea Meteorological Administration). These findings suggest that when CDW flows into southern KCWs on ocean currents during the summer season, typhoons play an important role in moderating the influence of CDW through strong water mixing; clearly this depends on the combination of the passage timing of typhoons in the East Asian region and the amount of the CRD.

4.2. Effect of CDW intrusion on C. polykrikoides blooms in southern KCWs

The geographical distribution and scale (area and duration) of *C. polykrikoides* blooms varied from year to year in KCWs. In particular, the *C. polykrikoides* blooms in 2010 and 2016 were small in area and short in duration, which corresponded with widespread expansion of CDW. In contrast, there were large-scale *C. polykrikoides* blooms in 2002 and 2014, which may have been related to limited spread of CDW. However, there were exceptions that deviated from these trends. The blooms in 2008, 2012, and 2014 were long in duration but small in area (average of 59 days and 2000 km^2, respectively), but in 2000 the bloom duration was short (29 days) but the area of spread was large (4200 km^2). These historical bloom reports indicate that it is difficult to explain the scale of *C. polykrikoides* blooms based on only one factor. The economic losses due to *C. polykrikoides* blooms, which are closely related to the scale of blooms, were positively correlated with bloom area ($p < 0.05$). In addition, the cumulative bloom area, a parameter that includes the bloom duration, showed a high correlation with economic losses compared with that for the daily bloom area (Hotelling's *t*-test; $t = 8.947$, $p < 0.01$), suggesting that it is necessary to incorporate both factors (area and duration) in estimating the scale of *C. polykrikoides* blooms.

The reduction in salinity in our study area, which occurred over an area >100,000 km^2, was mainly caused by large-scale expansion of CDW. Low salinity surface water can accelerate the formation of stratification, resulting in the development of a barrier layer, which reduces vertical mixing between warm surface water from cold deep water (Foltz and McPhaden, 2009; Godfrey and Lindstrom, 1989; Sprintall and Tomczak, 1992; Vialard and Delecluse, 1998). Interestingly, as a results of simulation studies using OGCM, it has been demonstrated that low-salinity CDW lead to the surface warming in East China Sea and Yellow Sea (Delcroix and Murtugudde, 2002; Park et al., 2011). The positive correlation between the sigma-t and the scale of *C. polykrikoides* blooms, including a trend of relatively small blooms during years of extensive expansion of CDW, indicates that massive intrusion of CDW has a negative effect on *C. polykrikoides* blooms. Numerous past reports of *C. polykrikoides* blooms have clarified the ranges of water temperature and salinity enabling the growth of this species. Thus, in East Asian regions blooms of this dinoflagellate mostly occur at >20 °C and salinities from 30 to 33 (Kudela and Gobler, 2012). In laboratory growth experiments, *C. polykrikoides* has been shown to grow well at 20–26 °C and salinities of 28–36, but has been reported to undergo stress under low salinity conditions at water temperatures >25 °C (Kim et al., 2004; Lim et al., 2019). Lim et al. (2019) reported that a *C. polykrikoides* strain did not grow at 30 °C even at salinity close to optimal for growth. High water temperature and low salinity (low sigma-t) are the main physicochemical properties of CDW, but these two factors varied significantly depending on the extent of intrusion of CDW ($p < 0.01$; Table 2). Thus, the average salinity in strong CDW years (29.38 ± 2.36) was significantly lower than in weak CDW years (31.3 ± 1.49), but even the lowest salinity in 2016 (28.02) was adequate for *C. polykrikoides* growth. On the other hand, in strong CDW years the mean water temperature of 27.95 ± 1.89 °C (maximum mean value in 2016: 28.91 °C) was beyond the optimum range for growth of *C. polykrikoides* (20–26 °C). Recent studies have demonstrated that abnormally high water temperature in the field, exceeding favorable growth conditions (approximately 30 °C), have a negative effect on *C. polykrikoides* blooms (Baek et al., 2020a; Lim et al., 2021). Together with these findings, since the lowered level of salinity can lead to surface warming, the intrusion strength of CDW may be a key factor, controlling *C. polykrikoides* blooms in KCWs.

In addition to salinity and water temperature, DO and NO_x concentrations also depended on the strength of intrusion of CDW (Table 2). The Changjiang River estuary is a very productive aquatic ecosystem, and this is directly related to the large amounts of nutrients in the river discharge (Ning et al., 2004). This discharge is the major source of terrestrial nutrients (mainly DIN) entering the East China Sea (Chen et al., 2010; Zhang, 1996), where an increasing N/P ratio in the surface layer generally causes the proliferation of diatoms (Hodgkiss and Ho, 1997). In general, diatoms, such as genera *Skeletonema*, *Chaetoceros*, and *Pseudo-nitzschia*, are dominant taxa in Changjiang River estuary during summer season (Jiang et al., 2015; Jiang et al., 2014; Qingshan et al., 2006). Based on previous studies, the satellite-estimated distributions of high Chl-*a* concentrations match well with that of CDW (Kim et al., 2009). In addition, satellite images for August 2018–2020 showed a similar pattern, in which high Chl-*a* concentrations originating from the Changjiang River estuary flowed into southern KCWs through CDW (Supplement 1). Similarly, the influx of phytoplankton communities in CDW may be responsible for the high DO concentrations in strong CDW years, despite the reduced oxygen solubility due to the high water temperature characteristics of CDW. The expansion of phytoplankton communities including diatoms carried by CDW may have negative effects on *C. polykrikoides* blooms. Based on Lim et al. (2014), diatoms *Skeletonema* and *Chaetoceros* showed a negative relationship with *C. polykrikoides*; these diatoms inhibited the growth and swimming ability of *C. polykrikoides*. In addition, it has been reported that the allelopathic effects tends to appear stronger in the unbalanced nutrient ratio (Granéli and Hansen, 2006; Granéli et al., 2008), and this N/P ratio in strong CDW years was significantly higher than weak CDW years ($p < 0.01$; 26 in strong CDW years >18 in weak CDW years). These findings suggest that the allelopathy of diatoms on *C. polykrikoides* may have synergistic effect depending on strength of CDW. Studies of the intrusion of phytoplankton with CDW, and their allelopathic effects on *C. polykrikoides*, are needed to assess this possibility. Negative effects on *C. polykrikoides* are also possible from other biological and chemical factors contained in CDW. For example, many previous studies have demonstrated algicidal bacterial effects on *C. polykrikoides* (Jeong et al., 2005; Jeong et al., 2003; Kim et al., 2008), and it is known that the concentrations of persistent organic pollutant (POPs) including organochlorine pesticides (e.g., DDTs, HCHs) are higher in the offshore area north of the Changjiang estuary compared to the southern area (Li et al., 2014). Consequently, physiochemical and biological changes associated with massive intrusion of CDW may be important in determining *C. polykrikoides* population dynamics. Further study of microbial and chemical components included in CDW is needed to assess their effects on HABs, including those caused by *C. polykrikoides*.

5. Summary

Based on environmental and red tide data covering approximately two decades, in this study a correlation was found between annual fluctuations in the intrusion of CDW into southern KCWs and the scale of

C. polykrikoides blooms. The annual volume of CDW (represented by the CRD) is mainly attributed to the ENSO, which controls the amount of precipitation falling in the Changjiang River catchment, but all of the CDW volume cannot be fully introduced into southern KCWs because of water mixing caused by typhoons during the inflow process. The scale of *C. polykrikoides* blooms was negatively correlated with the strength of the CDW intrusion. In addition, we found that it is possible to estimate the scale of *C. polykrikoides* blooms by considering both the bloom area and duration. Among the factors affected by massive intrusion of CDW, an increase in water temperature accelerated by low saline CDW is probably a major inhibitor of *C. polykrikoides* blooms. However, the influence of other biological and chemical factors in CDW may also influence bloom occurrence. Thus, in this study, the possibility that the conditions in CDW act to inhibit *C. polykrikoides* was confirmed. Further analysis of biomes and chemical s is necessary to clarify other factors inhibiting *C. polykrikoides* in CDW.

CRediT authorship contribution statement

Young Kyun Lim: Conceptualization, Formal analysis, Writing – original draft, Visualization. **Bum Soo Park:** Writing – review & editing, Validation. **Su Ho Bak:** Formal analysis, Writing – review & editing. **Sang-Soo Baek:** Writing – review & editing. **Seung Ho Baek:** Conceptualization, Funding acquisition, Writing – review & editing, Validation.

Declaration of Competing Interest

The authors declare that they have no known competing financial interests or personal relationships that could have appeared to influence the work reported in this paper.

Acknowledgements

This research was supported by the Ministry of Oceans and Fisheries of Korea [20210651; Techniques development for management and evaluation of biofouling on ship hulls] and the Ministry of Science, ICT & Future Planning [NRF-2016M1A5A1027456; the Basic Core Technology Development Program for the Oceans and the Polar Regions of the National Research Foundation], and the Korea Institute of Ocean Science and Technology (KIOST) [PEA0012; Biogeochemical cycling and marine environmental change study].

Appendix A. Supplementary data

Supplementary data to this article can be found online at https://doi.org/10.1016/j.ecolind.2022.108924.

References

Baek, S.H., Lee, M., Kim, Y.-B., 2018. Spring phytoplankton community response to an episodic windstorm event in oligotrophic waters offshore from the Ulleungdo and Dokdo islands, Korea. J. Sea Res. 132, 1–14.

Baek, S.H., Kim, Y., Lee, M., Ahn, C.-Y., Cho, K.H., Park, B.S., 2020a. Potential cause of decrease in bloom events of the harmful Dinoflagellate *Cochlodinium polykrikoides* in Southern Korean Coastal Waters in 2016. Toxins 12, 390.

Baek, S.H., Lee, M., Park, B.S., Lim, Y.K., 2020b. Variation in phytoplankton community due to an autumn typhoon and winter water turbulence in Southern Korean Coastal Waters. Sustainability 12, 2781.

Bai, Y., He, X., Pan, D., Chen, C.T.A., Kang, Y., Chen, X., Cai, W.J., 2014. Summertime Changjiang River plume variation during 1998–2010. J. Geophys. Res. Oceans 119, 6238–6257.

Chen, H., Yu, Z., Yao, Q., Mi, T., Liu, P., 2010. Nutrient concentrations and fluxes in the Changjiang Estuary during summer. Acta Oceanol. Sin. 29, 107–119.

Chen, Y.-l.L., Chen, H.-Y., Jan, S., Tuo, S.-h., 2009. Phytoplankton productivity enhancement and assemblage change in the upstream Kuroshio after typhoons. Mar. Ecol. Prog. Ser. 385, 111–126.

Delcroix, T., Murtugudde, R., 2002. Sea surface salinity changes in the East China Sea during 1997–2001: influence of the Yangtze River. J. Geophys. Res. Oceans. 107, 1–11.

Foltz, G.R., McPhaden, M.J., 2009. Impact of barrier layer thickness on SST in the central tropical North Atlantic. J. Clim. 22, 285–299.

Gao, B., Yang, D., Yang, H., 2013. Impact of the Three Gorges Dam on flow regime in the middle and lower Yangtze River. Quat. Int. 304, 43–50.

Godfrey, J., Lindstrom, E., 1989. The heat budget of the equatorial western Pacific surface mixed layer. J. Geophys. Res. Oceans. 94, 8007–8017.

Granéli, E., Hansen, P., 2006. Allelopathy in Harmful Algae: A Mechanism to Compete for Resources? Ecology of Harmful Algae. Springer, pp. 189–201.

Granéli, E., Weberg, M., Salomon, P.S., 2008. Harmful algal blooms of allelopathic microalgal species: the role of eutrophication. Harmful Algae 8, 94–102.

Hallegraeff, G.M., 2010. Ocean climate change, phytoplankton community responses, and harmful algal blooms: a formidable predictive challenge [1]. J. Phycol. 46, 220–235.

Hodgkiss, I., Ho, K., 1997. Are changes in N: P ratios in coastal waters the key to increased red tide blooms?. In: Asia-Pacific Conference on Science and Management of Coastal Environment. Springer, pp. 141–147.

Jeong, H., Yim, J.H., Lee, C., Choi, S.-H., Park, Y.K., Yoon, S.H., Hur, C.-G., Kang, H.-Y., Kim, D., Lee, H.H., 2005. Genomic blueprint of *Hahella chejuensis*, a marine microbe producing an algicidal agent. Nucleic Acids Res. 33, 7066–7073.

Jeong, S.-Y., Ishida, K., Ito, Y., Okada, S., Murakami, M., 2003. Bacillamide, a novel algicide from the marine bacterium, *Bacillus* sp. SY-1, against the harmful dinoflagellate, *Cochlodinium polykrikoides*. Tetrahedron Lett. 44, 8005–8007.

Jiang, Z., Liu, J., Chen, J., Chen, Q., Yan, X., Xuan, J., Zeng, J., 2014. Responses of summer phytoplankton community to drastic environmental changes in the Changjiang (Yangtze River) estuary during the past 50 years. Water Res. 54, 1–11.

Jiang, Z., Chen, J., Zhou, F., Shou, L., Chen, Q., Tao, B., Yan, X., Wang, K., 2015. Controlling factors of summer phytoplankton community in the Changjiang (Yangtze River) Estuary and adjacent East China Sea shelf. Cont. Shelf Res. 101, 71–84.

Kim, D.-I., Matsuyama, Y., Nagasoe, S., Yamaguchi, M., Yoon, Y.-H., Oshima, Y., Imada, N., Honjo, T., 2004. Effects of temperature, salinity and irradiance on the growth of the harmful red tide dinoflagellate *Cochlodinium polykrikoides* Margalef (Dinophyceae). J. Plankton Res. 26, 61–66.

Kim, D.-K., Kim, J.-H.-F., Yim, J.-H., Kwon, S.-K., Lee, C.-H., Lee, H.-K., 2008. Red to red-the marine bacterium *Hahella chejuensis* and its product prodigiosin for mitigation of harmful algal blooms. J. Microbiol. Biotechnol. 18, 1621–1629.

Kim, H.-C., Yamaguchi, H., Yoo, S., Zhu, J., Okamura, K., Kiyomoto, Y., Tanaka, K., Kim, S.-W., Park, T., Ishizaka, J., 2009. Distribution of Changjiang diluted water detected by satellite chlorophyll-a and its interannual variation during 1998–2007. J. Oceanogr. 65, 129–135.

Kudela, R.M., Gobler, C.J., 2012. Harmful dinoflagellate blooms caused by *Cochlodinium* sp.: global expansion and ecological strategies facilitating bloom formation. Harmful Algae 14, 71–86.

Lee, C.-K., Park, T.-G., Park, Y.-T., Lim, W.-A., 2013. Monitoring and trends in harmful algal blooms and red tides in Korean coastal waters, with emphasis on *Cochlodinium polykrikoides*. Harmful Algae 30, S3–S14.

Lee, D.-K., 2008. *Cochlodinium polykrikoides* blooms and eco-physical conditions in the South Sea of Korea. Harmful Algae 7, 318–323.

Lee, J.H., Moon, I., Moon, J., Kim, S., Jeong, Y.Y., Koo, J., 2017. Impact of typhoons on the Changjiang plume extension in the Yellow and East China Seas. J. Geophys. Res. Oceans 122, 4962–4973.

Lee, M.O., Kim, J.K., Kim, B.K., 2016. Factors controlling the origin of *Cochlodinium polykrikoides* blooms along the Goheung coast, South Korea. Mar. Pollut. Bull. 113, 165–175.

Lee, Y.S., 2006. Factors affecting outbreaks of high-density *Cochlodinium polykrikoides* red tides in the coastal seawaters around Yeosu and Tongyeong, Korea. Mar. Pollut. Bull. 52, 1249–1259.

Li, H., Dai, A., Zhou, T., Lu, J., 2010. Responses of East Asian summer monsoon to historical SST and atmospheric forcing during 1950–2000. Clim. Dyn. 34, 501–514.

Li, Y., Niu, J., Shen, Z., Zhang, C., Wang, Z., He, T., 2014. Spatial and seasonal distribution of organochlorine pesticides in the sediments of the Yangtze Estuary. Chemosphere 114, 233–240.

Lie, H.J., Cho, C.H., 1994. On the origin of the Tsushima Warm Current. J. Geophys. Res. Oceans 99, 25081–25091.

Lie, H.-J., Cho, C.-H., 2016. Seasonal circulation patterns of the Yellow and East China Seas derived from satellite-tracked drifter trajectories and hydrographic observations. Prog. Oceanogr. 146, 121–141.

Lim, A.S., Jeong, H.J., Jang, T.Y., Jang, S.H., Franks, P.J., 2014. Inhibition of growth rate and swimming speed of the harmful dinoflagellate *Cochlodinium polykrikoides* by diatoms: implications for red tide formation. Harmful Algae 37, 53–61.

Lim, A.S., Jeong, H.J., Jang, T.Y., Kang, N.S., Jang, S.H., Lee, M.J., 2015. Differential effects of typhoons on ichthyotoxic *Cochlodinium polykrikoides* red tides in the South Sea of Korea during 2012–2014. Harmful Algae 45, 26–32.

Lim, Y.K., Baek, S.H., Lee, M., Kim, Y.O., Choi, K.-H., Kim, J.H., 2019. Phytoplankton composition associated with physical and chemical variables during summer in the southern sea of Korea: implication of the succession of the two toxic dinoflagellates *Cochlodinium* (aka *Margalefidinium*) *polykrikoides* and *Alexandrium affine*. J. Exp. Mar. Biol. Ecol. 516, 51–66.

Lim, Y.K., Park, B.S., Kim, J.H., Baek, S.-S., Baek, S.H., 2021. Effect of marine heatwaves on bloom formation of the harmful dinoflagellate *Cochlodinium polykrikoides*: Two sides of the same coin? Harmful Algae 104, 102029.

Liu, X., Beusen, A.H., Van Beek, L.P., Mogollón, J.M., Ran, X., Bouwman, A.F., 2018. Exploring spatiotemporal changes of the Yangtze River (Changjiang) nitrogen and phosphorus sources, retention and export to the East China Sea and Yellow Sea. Water Res. 142, 246–255.

Matsuno, T., Lee, J.S., Shimizu, M., Kim, S.H., Pang, I.C., 2006. Measurements of the turbulent energy dissipation rate and an evaluation of the dispersion process of the Changjiang Diluted Water in the East China Sea. J. Geophys. Res. Oceans 111, C11S09.

Ning, X., Shi, J., Cai, Y., Liu, C., 2004. Biological productivity front in the Changjiang Estuary and the Hangzhou Bay and its ecological effects. Acta Oceanol. Sin. 26, 96–106.
Paerl, H.W., Rossignol, K.L., Hall, S.N., Peierls, B.L., Wetz, M.S., 2010. Phytoplankton community indicators of short-and long-term ecological change in the anthropogenically and climatically impacted Neuse River Estuary, North Carolina, USA. Estuaries Coast 3, 485–497.
Park, J., Kwon, Y.S., Baek, S.H., Lim, W.A., Park, J., Jang, J., Park, Y., 2019. Identifying Environmental Effects on an Annual Variation in *Margalefidinium polykrikoides* in the South Korean Sea Using Statistical Analysis. J. Coast. Res. 90, 11–18.
Park, T., Jang, C.J., Jungclaus, J.H., Haak, H., Park, W., 2011. Effects of the Changjiang river discharge on sea surface warming in the Yellow and East China Seas in summer. Cont. Shelf Res. 31, 15–22.
Park, T., Jang, C.J., Kwon, M., Na, H., Kim, K.-Y., 2015. An effect of ENSO on summer surface salinity in the Yellow and East China Seas. J. Mar. Syst. 141, 122–127.
Park, T.G., Lim, W.A., Park, Y.T., Lee, C.K., Jeong, H.J., 2013. Economic impact, management and mitigation of red tides in Korea. Harmful Algae 30, S131–S143.
Qingshan, L., Jun, S., Zhiliang, S., Shuqun, S., Min, W., 2006. Phytoplankton assemblage of Yangtze River Estuary and the adjacent East China Sea in summer, 2004. J. Ocean Univ. China 5, 123–131.
Sprintall, J., Tomczak, M., 1992. Evidence of the barrier layer in the surface layer of the tropics. J. Geophys. Res. Oceans. 97, 7305–7316.
Suh, H., Cho, Y., Soh, Y., Kim, D., 1998. The 1996 mass mortality of macrobenthic animals in Cheju Island: a possible role of physical oceanographic factor. Kor. J. Environ. Biol 17, 175–182.
Vialard, J., Delecluse, P., 1998. An OGCM study for the TOGA decade. Part I: Role of salinity in the physics of the western Pacific fresh pool. J. Phys. Oceanogr. 28, 1071–1088.
Wei, H., Luo, X., Zhao, Y., Zhao, L., 2015. Intraseasonal variation in the salinity of the Yellow and East China Seas in the summers of 2011, 2012, and 2013. Hydrobiologia 754, 13–28.
Wells, M.L., Trainer, V.L., Smayda, T.J., Karlson, B.S., Trick, C.G., Kudela, R.M., Ishikawa, A., Bernard, S., Wulff, A., Anderson, D.M., 2015. Harmful algal blooms and climate change: Learning from the past and present to forecast the future. Harmful Algae 49, 68–93.
Zhang, J., 1996. Nutrient elements in large Chinese estuaries. Cont. Shelf Res. 16, 1023–1045.
Zhang, Z., Wu, H., Yin, X., Qiao, F., 2018. Dynamical response of Changjiang River plume to a severe typhoon with the surface wave-induced mixing. J. Geophys. Res. Oceans. 123, 9369–9388.
Zheng, G.M., Tang, D., 2007. Offshore and nearshore chlorophyll increases induced by typhoon winds and subsequent terrestrial rainwater runoff. Mar. Ecol. Prog. Ser. 333, 61–74.
Zhou, T., Zhang, L., Li, H., 2008. Changes in global land monsoon area and total rainfall accumulation over the last half century. Geophys. Res. Lett. 35, L16707.